Quasiparticles of a periodically driven quantum dot coupled between superconducting and normal leads

B. Baran* and T. Domański†
Institute of Physics, M. Curie-Skłodowska University, 20-031 Lublin, Poland

(Received 7 May 2019; revised manuscript received 16 July 2019; published 9 August 2019)

We investigate subgap quasiparticles of a quantum dot coupled to the superconducting and normal leads, whose energy level is periodically driven by an external potential. Using the Floquet formalism we determine the quasienergies and analyze redistribution of their spectral weights between individual harmonics upon varying the frequency and amplitude of the driving potential. We propose feasible spectroscopic methods for probing the in-gap quasiparticles observable in the differential conductance of the charge current averaged over a period of oscillations.

DOI: 10.1103/PhysRevB.100.085414

I. MOTIVATION

Response of a quantum system on abrupt quench [1] or periodically driven perturbation [2] can provide valuable insight into dynamics of its effective quasiparticles or may even lead to appearance of novel phases [3,4]. Among numerous examples one can mention, e.g., quantum time crystals [5], transient engineering of superconductivity [6], light-induced coherence in atomic superfluids [7], insulating [8] or superconducting topological phases [9–11], zero and π modes in planar Josephson junctions [12], and many other effects in the solid state [13–16], quantum optics [17,18], nanostructures [19,20], or ultracold gases [21–23].

In nanoscopic heterostructures such phenomena affect the charge and spin transport, therefore it could be promising for future applications. In particular, very interesting effects can be observed at impurities hybridized with superconductors, where the bound Andreev (or Yu-Siba-Rusinov) states appear in the subgap regime. Upon perturbing such impurities by external periodic field they absorb or emit the field quanta, inducing the higher-order harmonics. These features have been indeed reported experimentally [24,25], but their detailed knowledge is not well established yet. Subgap quasiparticles involve the particle and hole degrees of freedom, one may hence ask *whether the Andreev (Yu-Shiba-Rusinov) states shall split into a series of equidistant harmonics, or rather the quasienergies of the normal (unpaired) quantum impurity would undergo internal splittings*. We try to answer this question, considering the setup (Fig. 1) of the single quantum dot strongly coupled to the superconductor and weakly hybridized with the normal lead. Energy level of this quantum dot can be periodically driven either by electromagnetic field or by alternating gate potential.

The charge and heat transport through similar heterostructure has been recently discussed by Arrachea and López [26], but specific quasienergies of this setup have not been investigated. Multiple in-gap features originating from AC field [27] or the coupling to monochromatic boson field have been also explored by several other groups [28–31], however the role of frequency and amplitude of external perturbations have not been treated on equal footing. For this reason we address such an issue here, investigating the quasienergies and their spectral weights driven in the proximitized dot by external perturbation.

The paper is organized as follows. We define the microscopic model in Sec. II and discuss methodological details to treat the periodic driving in Sec. III. Our main results are presented in Sec. IV. Section V summarizes the major conclusions and gives a brief outlook of open questions. In Appendix A we illustrate the Floquet formalism applied to the normal (unpaired) quantum dot and in Appendix B we present the effective model obtained for the high-frequency limit.

II. MICROSCOPIC MODEL

The setup comprising the quantum dot (QD) coupled to the normal (N) and superconducting (SC) reservoirs can be described by the Anderson impurity Hamiltonian

$$H(t) = H_{\rm QD}(t) + H_{\rm N} + H_{\rm SC} + H_{T,\rm N} + H_{T,\rm SC}. \tag{1}$$

Time dependence enters our setup through

$$H_{\rm QD}(t) = \sum_{\sigma} \varepsilon_d(t) d_\sigma^\dagger d_\sigma, \tag{2}$$

where we assume periodic oscillations of the QD energy level $\varepsilon_d(t) = \varepsilon_d + A\cos(\omega t)$. As usual, $d_\sigma^{(\dagger)}$ stands for the creation (annihilation) operator of the QD electrons with spin $\sigma = \{\uparrow, \downarrow\}$. Oscillations of the energy level $\varepsilon_d(t)$ are characterized by frequency ω and amplitude A. We assume that they have no direct influence on electronic states of both external leads which are described by

$$H_{\rm N} = \sum_{k\sigma} \xi_{{\rm N}k}\, c_{{\rm N}k\sigma}^\dagger\, c_{{\rm N}k\sigma}, \tag{3}$$

$$H_{\rm SC} = \sum_{k\sigma} \xi_{{\rm SC}k}\, c_{{\rm SC}k\sigma}^\dagger\, c_{{\rm SC}k\sigma} - \sum_{k} (\Delta\, c_{{\rm SC}k\uparrow}^\dagger\, c_{{\rm SC}-k\downarrow}^\dagger + {\rm H.c.}). \tag{4}$$

*bartlobaran@kft.umcs.lublin.pl
†doman@kft.umcs.lublin.pl

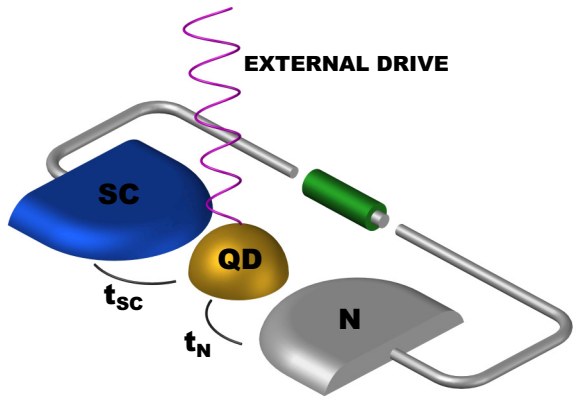

FIG. 1. Schematics of the externally driven quantum dot (QD) hybridized with superconducting (SC) and normal (N) electrodes by couplings t_{SC} and t_N, respectively.

Here $c^\dagger_{\beta k\sigma}$ ($c_{\beta k\sigma}$) are the creation (annihilation) operators of itinerant electrons with spin σ and momentum k in $\beta = $ N and SC electrodes. The energy gap of isotropic superconducting reservoir is denoted by Δ. The energies $\xi_{\beta k} = \varepsilon_{\beta k} - \mu_\beta$ are measured with respect to the chemical potentials μ_β, which can be detuned $\mu_n - \mu_s = eV$ by applying the bias V. The last terms of Hamiltonian (1) stand for hybridization of the QD with external leads

$$H_{T,\beta} = \sum_{k\sigma} (t_\beta c^\dagger_{\beta k\sigma} d_\sigma + t^*_\beta d^\dagger_\sigma c_{\beta k\sigma}). \tag{5}$$

In what follows, we study the quasiparticle states appearing inside the energy regime $|E| \leqslant \Delta$, assuming both hybridizations t_β to be constant (momentum independent). Signatures of periodic driving appearing outside the gap are briefly addressed in Sec. IV D.

III. METHODOLOGY

Quantum systems described by the time-periodic Hamiltonians $H(t) = H(t+T)$, where $T = 2\pi/\omega$ can be treated within the Floquet formalism. An outline of this procedure is presented in Appendix A for the nonsuperconducting case. Here we apply this treatment to the setup, where the proximity induced on-dot pairing mixes the particle with hole degrees of freedom. Let us discuss how to treat such effects in the presence of the periodic driving.

Quasiparticle spectrum and transport properties of the N-QD-S setup can be obtained using the Green's function approach [32] combined with the Floquet technique [33,34] to account for the periodically oscillating QD level. Since a proximity effect induces the on-dot pairing we introduce the matrix (Nambu) representation

$$G^\nu_{d,d}(t,t') = \begin{pmatrix} \langle\langle d_\uparrow(t); d^\dagger_\uparrow(t')\rangle\rangle & \langle\langle d_\uparrow(t); d_\downarrow(t')\rangle\rangle \\ \langle\langle d^\dagger_\downarrow(t); d^\dagger_\uparrow(t')\rangle\rangle & \langle\langle d^\dagger_\downarrow(t); d_\downarrow(t')\rangle\rangle \end{pmatrix}, \tag{6}$$

where the upper index ν stands either for the retarded ($\nu = r$), advanced ($\nu = a$), or Keldysh ($\nu = c$) Green's functions. The Heisenberg equation of motion yields

$$G^\nu_{d,d}(t,t') = g^\nu_{d,d}(t,t') + \int dt_1 \sum_{k,\beta} g^\nu_{d,d}(t,t_1) t^*_\beta G^\nu_{\beta k,d}(t_1,t'), \tag{7}$$

where $g^\nu_{d,d}(t,t')$ is the (bare) Green's function of isolated QD, whereas $G^\nu_{\beta k,d}(t_1,t')$ denotes the mixed function originating from hybridization of the QD with itinerant electrons of external ($\beta = $ N, SC) leads. Equation of motion for this mixed Green's function $G^\nu_{\beta k,d}(t_1,t')$ yields

$$G^\nu_{d,d}(t,t') = g^\nu_{d,d}(t,t') + \int dt_1 \int dt_2 \sum_\beta g^\nu_{d,d}(t,t_1)\mathbf{\Sigma}^\nu_\beta \times (t_1,t_2) G^\nu_{d,d}(t_2,t'), \tag{8}$$

with the self-energy matrix

$$\mathbf{\Sigma}^\nu_\beta(t_1,t_2) = \sum_k |t_\beta|^2 g^\nu_{\beta k,\beta k}(t_1,t_2). \tag{9}$$

All Green's functions and the self-energies depend on two-time arguments t and t', but such dependence can be substantially simplified owing to the discrete translational invariance $f(t,t') = f(t+nT, t'+mT)$ where n and m are integer numbers. In what follows, we restrict our considerations to the steady limit.

Time periodicity can be conveniently treated, by transforming t, t' to the relative $t - t'$ and average time $(t+t')/2$ arguments and introducing the Wigner transformation [33]. We follow a slightly different convention [35], introducing the transformation

$$f_{nm}(\epsilon) = \int_{-\infty}^{\infty} dt' \frac{1}{T} \int_0^T dt e^{i(\epsilon+n\omega)t - i(\epsilon+m\omega)t'} f(t,t'), \tag{10}$$

with the quasienergy ϵ. This allows us to recast time convolutions appearing in Eqs. (7) and (8) by summations over the discrete harmonics m, n and integral over the first Floquet zone $\epsilon \in \langle -\omega/2; \omega/2\rangle$.

We can next diagonalize the bare Green's function $(g^\nu_{d,d}(\epsilon))^{-1}_{nm}$ with respect to the Floquet coordinates n, m by the appropriate unitary matrix $\Lambda_{nl}(\varepsilon) = (\Lambda_{nl}(\varepsilon))^\dagger$,

$$\sum_{nm} \Lambda_{ln}(\epsilon) \big(g^\nu_{d,d}(\epsilon)\big)^{-1}_{nm} \Lambda^\dagger_{ml}(\epsilon) = \big(Q^\nu_{d,d}(\epsilon)\big)^{-1}_{ll}. \tag{11}$$

In this basis the retarded and advanced Green's function are simply expressed by

$$\big(Q^{r,a}_{d,d}(\epsilon)\big)^{-1}_{ll} = (\epsilon + l\omega \pm i\eta^+) I - \varepsilon^0_d \tau_z, \tag{12}$$

where I stands for the identity matrix, τ_z denotes z component of the Pauli matrix, and $i\eta^+$ is an infinitesimal positive imaginary value. Since we have chosen the time-dependent QD level $\varepsilon_d(t)$ of a cosine form, the diagonalizing basis defined through (11) is expressed by the Bessel functions of a first kind [36]

$$\Lambda_{nl}(\epsilon) = \frac{1}{T}\int_0^T dt e^{i(n-m)\epsilon t}\, e^{-i\int_0^t dt'[\varepsilon_d(t') - \varepsilon_d(0)]} = J_{n-m}\left(\frac{A}{\omega}\right). \tag{13}$$

Due to completeness of the Bessel functions, we can express the bare Green's function in the following form:

$$\left(g^{r/a}_{d,d}(\epsilon)\right)_{nm} = \sum_l \begin{pmatrix} \frac{J_{n-l}(A/\omega)J_{m-l}(A/\omega)}{\epsilon \pm i\eta^+ + l\omega - \varepsilon_d^0} & 0 \\ 0 & \frac{J_{n-l}(A/\omega)J_{m-l}(A/\omega)}{\epsilon \pm i\eta^+ + l\omega + \varepsilon_d^0} \end{pmatrix}. \tag{14}$$

Detailed derivation of such transformation has been discussed, e.g., in Refs. [33,35].

In the same way we express the self-energies (9) originating from hybridization of the QD with external leads

$$\left(\Sigma^{r/a}_{\beta}(\epsilon)\right)_{nm} = \sum_k |t_\beta|^2 \left(g^{r/a}_{\beta k,\beta k}(\epsilon)\right)_{nm}. \tag{15}$$

We are mainly interested in the subgap quasiparticles, therefore we make use of the wide-band limit approximation [37], introducing the constant couplings $\Gamma_\beta \simeq 2\pi |t_\beta|^2 \rho(\mu_\beta)$ which relies on the assumption that the densities of states $\rho(\epsilon_{\beta k})$ of both electrodes are nearly constant within the energy regime $\epsilon_{\beta k}$ smaller or comparable to Δ around the chemical potentials μ_β. In the Floquet's space the self-energies become diagonal. The normal term is simply given as

$$\left(\Sigma^{r/a}_{N}(\epsilon)\right)_{nm} = \mp \begin{pmatrix} \frac{i\Gamma_N}{2} & 0 \\ 0 & \frac{i\Gamma_N}{2} \end{pmatrix} \delta_{nm}, \tag{16}$$

whereas the superconducting contribution is nondiagonal in the Nambu representation [26,38]

$$\left(\Sigma^{r/a}_{\rm SC}(\epsilon)\right)_{nm} = -\frac{\alpha(\tilde{\varepsilon})\,\Gamma_{\rm SC}/2}{\sqrt{|(\tilde{\varepsilon} \pm i\eta^+)^2 - \Delta^2|}} \begin{pmatrix} \tilde{\varepsilon} & -\Delta \\ -\Delta & \tilde{\varepsilon} \end{pmatrix} \delta_{nm}, \tag{17}$$

where $\alpha(\tilde{\epsilon}) = \Theta(\Delta - |\tilde{\epsilon}|) \pm i\,\mathrm{sgn}(\tilde{\epsilon})\Theta(|\tilde{\epsilon}| - \Delta)$ and $\tilde{\epsilon} = \epsilon + n\omega$. The self-energy (17) is responsible for the pairing effects manifested in the effective quasiparticle spectrum.

IV. EFFECTIVE SPECTRUM

In what follows we present representative numerical results obtained for the periodically oscillating quantum dot, assuming $\varepsilon_d = 0$, $\Gamma_{\rm N} = 0.1\Gamma_{\rm SC}$, and focusing on the zero temperature limit. Our main interests are the subgap quasiparticles and efficiency of the induced on-dot electron pairing, we therefore consider first the superconducting atomic limit $\Delta \to \infty$ when the self-energy (17) simplifies to its static value [39]. Role of the finite energy gap Δ is discussed in Sec. IV D.

A. In-gap quasiparticles

The effective QD spectrum driven by oscillations of the energy level $\varepsilon_d(t)$ can be characterized by the diagonal (in Nambu representation) spectral function

$$\langle \rho_d(\epsilon) \rangle = \sum_n \left(-\frac{1}{\pi} \mathrm{Im}\left[G^r_{d,d}(\epsilon + i0^+) \right]_{1,1} \right)_{nn} \tag{18}$$

of the electron propagator $\langle\langle d_\uparrow(t); d^\dagger_\uparrow(t')\rangle\rangle$ whose Fourier transform is defined in Eq. (10). Influence of the normal and superconducting reservoirs affect this propagator via the Dyson equation (8). Trace over the Floquet indices is here equivalent to averaging over a single period T. Such a spectral

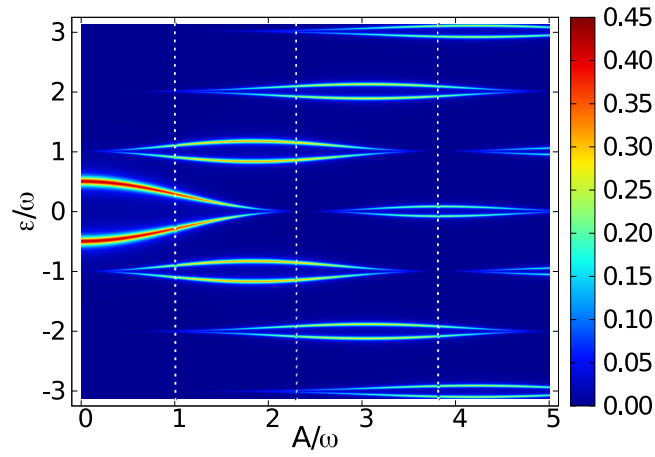

FIG. 2. The diagonal spectral function (18) of the quantum dot driven by periodic oscillations of its initial level $\varepsilon_d = 0$, assuming $\Gamma_{\rm SC}/\omega = 1$ and $\Gamma_{\rm N}/\omega = 0.1$.

function for an arbitrary physical problem has been recently shown to always take the positive values [40]. For convenience we normalize this function (18), multiplying it by $c = \frac{\pi}{2}\Gamma_{\rm N}$. In the time-independent case ($A = 0$ or $\omega = 0$) this would imply $c\langle\rho_d(\epsilon)\rangle \to 1$ for ε coinciding with the Andreev bound states energy.

The normal QD (see Appendix A) is characterized by a series of equidistant harmonics $\varepsilon_d + n\omega$ (where n stands for positive and negative integer numbers) whose spectral weights vary with the amplitude A. This structure changes qualitatively when the proximity induced on-dot pairing is taken into account. Figure 2 shows the averaged spectral function (18) as a function of the quasienergy ε and amplitude A obtained for $\Gamma_{\rm SC}/\omega = 1$. We can notice that the normal quantum dot quasienergies $\varepsilon_d + n\omega$ split into the lower and upper branches.

Let us analyze this spectrum in more detail. In the stationary case the subgap spectrum consists of a pair of the Andreev bound states at $\pm\sqrt{\varepsilon_d^2 + (\Gamma_{\rm SC}/2)^2}$ [39]. For our present configuration they acquire some finite line broadening (inverse lifetime) originating from the coupling $\Gamma_{\rm N}$ to a continuum of the normal lead electrons. Upon increasing the amplitude A the quasiparticle branches (corresponding to $n = 0$) gradually approach each other, and simultaneously the higher-order harmonics $|n| \geqslant 1$ are developed. Each of such higher-order quasiparticle branches reveal also the splitting but its magnitude gets smaller and smaller with increasing n. The averaged spectrum (Fig. 2) clearly displays that such harmonics do not mix between themselves. They rather show an "avoided crossing" behavior.

Such variation of the quasiparticle energies with respect to A is accompanied by considerable redistribution of their spectral weights. We observe that each of the harmonics gain and lose their weights upon varying the amplitude in roughly the same fashion as for the normal quantum dot (see Appendix A). Figure 3 illustrates the averaged spectral function versus the frequency ω of oscillations obtained for $A = 2.2\Gamma_{\rm SC}$. Here we notice that quasiparticle energies and ongoing transfer of their spectral weights between different harmonics at larger frequencies produce the spectrum comprising the higher order states near $\varepsilon_d + n\omega$ (like in the normal case) and one pair (of

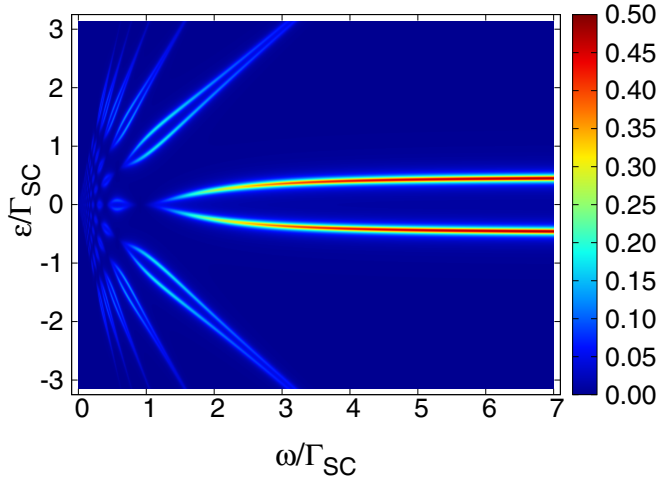

FIG. 3. Variation of the the averaged quasiparticle spectrum with respect to the frequency ω obtained for the constant amplitude $A = 2.2\Gamma_{\rm SC}$, assuming $\varepsilon_d = 0$ and $\Gamma_{\rm N} = 0.1\Gamma_{\rm SC}$.

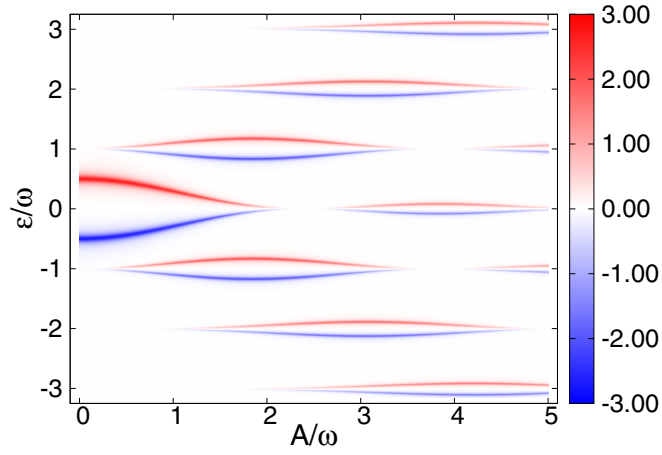

FIG. 4. The averaged off-diagonal spectral function (19) obtained for the same set of model parameters as in Fig. 2.

zeroth order) Andreev quasiparticles. Numerical data obtained in the high frequency limit are consistent with the analytical results derived from the Magnus expansion (discussed in Appendix B).

B. Induced on-dot pairing

To characterize efficiency of the proximity induced on-dot pairing we introduce the off-diagonal (in Nambu space) spectral function

$$\langle \rho_{\rm off}(\epsilon)\rangle = \sum_n \left(-\frac{1}{\pi}{\rm Im}\big[G^r_{d,d}(\epsilon + i0^+)\big]_{1,2}\right)_{nn} \tag{19}$$

related to the anomalous propagator $\langle\langle d^\dagger_\uparrow(t); d^\dagger_\downarrow(t')\rangle\rangle$ describing probability of creating the pair of opposite spin electrons. This anomalous propagator has a number of properties typical for bosonic objects. In bulk and nanoscopic superconductors under the static conditions ($A = 0$) one of them is manifested by the symmetry relation $[G^r_{d,d}(-\epsilon + i0^+)]_{1,2} = [G^r_{d,d}(\epsilon + i0^+)]^*_{1,2}$ that implies the odd spectral function $\rho_{\rm off}(-\epsilon) = -\rho_{\rm off}(\epsilon)$. More detailed discussion of the superconducting features of the proximitized/correlated QDs has been presented, e.g., in Refs. [39,41]. For the periodically driven system ($A \neq 0$), we notice here similar relationship valid also for the higher harmonics $|n| > 0$. Figure 4 shows the off-diagonal spectral function (19) with respect to the varying amplitude A. The anomalous spectral function is indeed reminiscent of the behavior displayed in Fig. 2, except that now the upper and lower branches of individual harmonics have opposite signs.

We can also determine expectation value of the on-dot pairing potential $\langle d_\downarrow d_\uparrow\rangle_T$ averaged over a period T. Its dependence on the amplitude A is presented in Fig. 5. This induced order parameter seems to be predominately sensitive to the amount of spectral weight of the zeroth order harmonic states (it vanishes for such amplitude where the zero-level harmonic states lose their spectral weights). In the next section we shall check whether the quasiparticle spectrum and/or the induced on-dot pairing could be observable experimentally by the tunneling current measurements.

C. Subgap charge current

Quasiparticle spectrum of the quantum dot could be probed only indirectly through the transport properties. Let us briefly discuss how to determine the time-dependent charge current and its differential conductance. We focus on an adiabatic limit and use the Landauer's technique to describe the current induced in our setup by a small bias V, which detunes the chemical potentials $\mu_{\rm N} = \mu_{\rm SC} + eV$. To be specific, we assume the superconducting lead to be grounded $\mu_{\rm SC} = 0$.

The charge current flowing from βth electrode $I_\beta(t) = e\langle \dot{N}_\beta(t)\rangle$ can be expressed by [27]

$$I_\beta(t) = \frac{2e}{\hbar}\int dt_1 {\rm Re}\big[G^r_{d,d}(t,t_1)\Sigma^<_\beta(t_1,t) + G^<_{d,d}(t,t_1)\Sigma^a_\beta(t_1,t)\big]_{11-22}, \tag{20}$$

where factor 2 accounts for contributions from both spins, whereas the diagonal elements {11} and {22} correspond to the particle and hole terms, respectively. In the Floquet's space

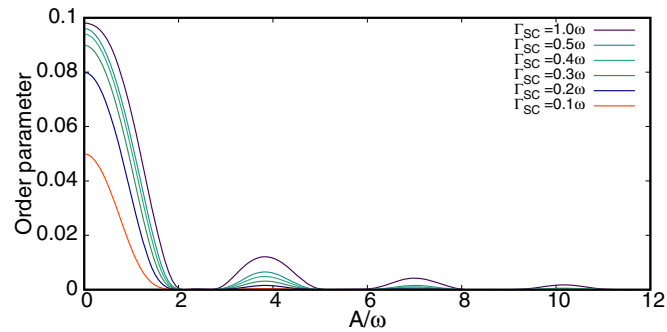

FIG. 5. Expectation value of the proximity induced order parameter $\langle d_\downarrow d_\uparrow\rangle$ versus the amplitude A obtained for $\varepsilon_d = 0$, $\Gamma_{\rm N}/\omega = 0.1$ and several values of $\Gamma_{\rm SC}$, as indicated.

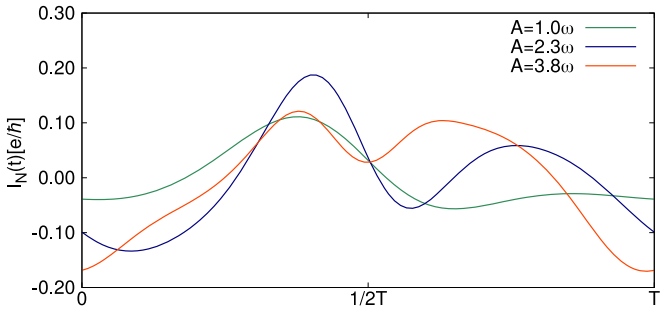

FIG. 6. Time-dependent current $I_{\rm N}(t)$ obtained for $V = 1\omega$, assuming $\varepsilon_d = 0$ and the couplings $\Gamma_{\rm SC} = 1\omega$, $\Gamma_{\rm N} = 0.1\omega$.

we can recast Eq. (20) to the form

$$I_\beta(t) = \frac{2e}{\hbar}\int_{-\omega/2}^{\omega/2} d\epsilon \sum_{n,m,p} \mathrm{Re}\big\{e^{-i(n-p)\omega t}\big[\big(G^r_{d,d}(\epsilon)\big)_{nm} \times(\Sigma^<_\beta(\epsilon))_{mp} + (G^<_{d,d}(\epsilon))_{nm}(\Sigma^a_\beta(\epsilon))_{mp}\big]_{11-22}\big\}. \tag{21}$$

We have computed numerically the time-dependent current (21) for several amplitudes A marked by the dashed lines in Fig. 2. The current $I_{\rm N}$ obtained for the bias voltage $V = 1\omega/e$ (where e denotes elementary charge) within a single period T is displayed in Fig. 6. For an opposite bias the symmetry relation $I_{\rm N}(-V,t) = -I_{\rm N}(V, t+\frac{T}{2})$ can be used. In general, we hardly find any relevance of such time-dependent charge currents to effective quasiparticle spectrum of the driven quantum dot.

In order to get some correspondence with the effective QD spectrum let us analyze the transport properties averaged over the single period T. The averaged charge current can be obtained from (21):

$$\langle I_\beta\rangle = \frac{2e}{\hbar}\int_{-\omega/2}^{\omega/2} d\epsilon \sum_{n,m} \mathrm{Re}\big\{\big[\big(G^r_{d,d}(\epsilon)\big)_{nm}(\Sigma^<_\beta(\epsilon))_{mn} + (G^<_{d,d}(\epsilon))_{nm}\big(\Sigma^a_\beta(\epsilon)\big)_{mn}\big]_{11-22}\big\}. \tag{22}$$

We can express the lesser Green's function $(G^<_{d,d}(\epsilon))_{nm}$ by convolutions of the retarded and advanced Green's functions, which in the mixed Nambu/Floquet notations take the following structure [27]:

$$\begin{aligned}[(G^<_{d,d}(\epsilon))_{nm}]_{\mu\nu} &= \sum_{kl}\big\{\big[\big(G^r_{d,d}(\epsilon)\big)_{nk}\big]_{\mu 1}[(\Sigma^<(\epsilon))_{kl}]_{11}\big[\big(G^a_{d,d}(\epsilon)\big)_{lm}\big]_{1\nu} \\ &+ \big[\big(G^r_{d,d}(\epsilon)\big)_{nk}\big]_{\mu 1}[(\Sigma^<(\epsilon))_{kl}]_{12}\big[\big(G^a_{d,d}(\epsilon)\big)_{lm}\big]_{2\nu} \\ &+ \big[\big(G^r_{d,d}(\epsilon)\big)_{nk}\big]_{\mu 2}[(\Sigma^<(\epsilon))_{kl}]_{21}\big[\big(G^a_{d,d}(\epsilon)\big)_{lm}\big]_{1\nu} \\ &+ \big[\big(G^r_{d,d}(\epsilon)\big)_{nk}\big]_{\mu 2}[(\Sigma^<(\epsilon))_{kl}]_{22}\big[\big(G^a_{d,d}(\epsilon)\big)_{lm}\big]_{2\nu}\big\},\end{aligned} \tag{23}$$

where $\mu, \nu \in \{1, 2\}$. The lesser self-energy matrix

$$\Sigma^<(\epsilon) = \Sigma^<_{\rm N}(\epsilon) + \Sigma^<_{\rm SC}(\epsilon) \tag{24}$$

can be given by

$$(\Sigma^<_\beta(\epsilon))_{nm} = \big[\big(\Sigma^a_\beta(\epsilon)\big)_{nm} - \big(\Sigma^r_\beta(\epsilon)\big)_{nm}\big] f_\beta(\epsilon + n\omega), \tag{25}$$

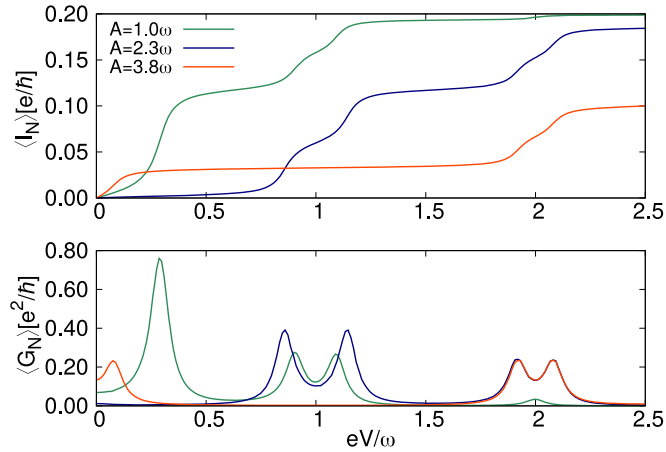

FIG. 7. The averaged current $\langle I_{\rm N}\rangle$ and differential conductance $\langle G_{\rm N}\rangle$ versus the applied bias voltage V determined from the Floquet's treatment for $\Gamma_{\rm SC} = 1\omega$, $\Gamma_{\rm N} = 0.1\omega$, and $\varepsilon_d = 0$.

where $f_\beta(x) = 1/[e^{(x-\mu_\beta)/k_BT} + 1]$ is the Fermi-Dirac distribution function for electrons in βth lead.

We have computed the averaged current given by Eq. (22) for the same set of parameters as discussed in Figs. 2 and 4. Under equilibrium conduction the net current $\langle I_\beta\rangle$ vanishes, because incoming and outgoing charge transfers cancel each other. Figure 7 shows the averaged charge current (top panel) and its differential conductance (bottom panel) as functions of the applied voltage V for three amplitudes of the oscillations, as indicated. Enhancements of the differential conductance perfectly coincide with the energy dependent subgap quasiparticles (presented in Fig. 8) with the correspondence $\varepsilon \leftrightarrow eV$.

Differential conductance of the charge current averaged over a period of the oscillations would thus experimentally probe the effective quasiparticle spectrum, revealing the splittings of all harmonic levels.

D. Finite Δ effects

In realistic situations the energy gap Δ is finite, usually on the order of a few or fractions of meV. Let us inspect influence of such threshold on the effective quasiparticle spectrum. For specific computations we use $\Delta = 0.5\omega$, when

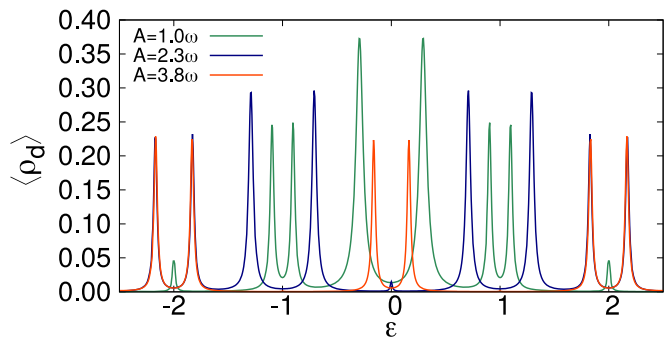

FIG. 8. Profiles of the diagonal spectral function (18) obtained for three amplitudes of oscillations, as indicated.

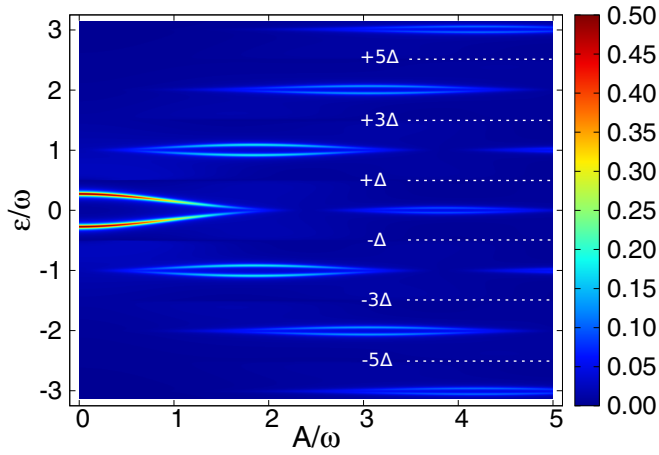

FIG. 9. Effective quasiparticle states obtained for $\Delta = 0.5\omega$, assuming $\varepsilon_d = 0$, $\Gamma_{\rm SC} = 1\omega$, and $\Gamma_{\rm N} = 0.1\omega$.

the higher-order harmonics $|n| \neq 0$ are pushed outside the superconducting energy gap window.

Figure 9 presents the quasiparticle spectrum with respect to the varying amplitude A. In comparison to the limit $\Delta \to \infty$, we notice that outside the superconducting gap the splitting of each harmonics substantially diminishes. This is rather well expected behavior, but in addition we also observe further qualitative changes. When the amplitude A exceeds the superconducting gap a partial leakage of the spectral weight occurs towards the in-gap regime. It appears in the form of continuous background, corresponding to incoherent subgap states.

Figure 10 illustrates distribution of the spectral weight between the multiple harmonics, revealing their splittings and the presence of the incoherent in-gap states. Let us notice that for sufficiently fast oscillations we practically obtain the ordinary (zero-level) Andreev quasiparticle states, whereas all the rest of the spectrum is far outside the energy gap, arranged into the higher order modes $\varepsilon_d \pm n\omega$. Vicinity of the higher order harmonics is partly depleted from its continuous states—this is exactly an opposite tendency to the leakage of incoherent background displayed in Fig. 9. This finite value of the superconducting energy gap is here manifested in a unique manner, without analogy to the static situations.

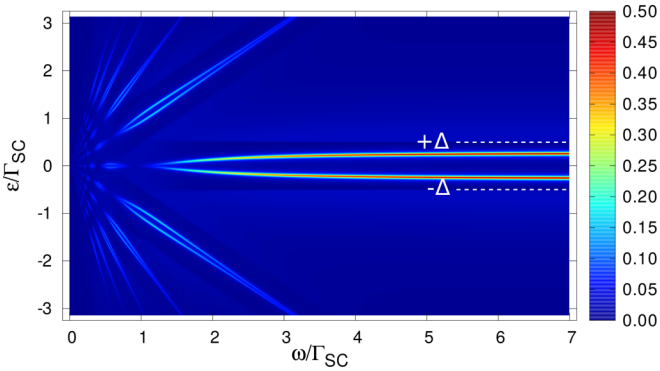

FIG. 10. Quasiparticle spectrum of the driven quantum dot obtained for the finite superconducting energy gap $\Delta = 0.5\Gamma_{\rm SC}$, assuming $\varepsilon_d = 0$, $\Gamma_{\rm N} = 0.1\Gamma_{\rm SC}$, and $A = 2.2\Gamma_{\rm SC}$.

V. SUMMARY AND OUTLOOK

We have studied an effective spectrum of the single level quantum dot sandwiched between the superconducting and metallic electrodes and periodically driven by an external potential. We have analyzed variations of its quasienergies and spectral weights with respect to the frequency ω and the amplitude A of oscillations. In contrast to the normal case (characterized by equidistant quasienergies $\varepsilon_d + n\omega$) we find that the proximity induced electron pairing leads to the splitting of each harmonic level. Such splitting is mostly pronounced in the zeroth harmonic state and gradually ceases in the higher harmonics. Distribution of the spectral weight between these harmonic quasienergies is controlled by the amplitude to frequency ratio.

We have inspected the charge transport properties, establishing that the effective quasiparticle spectrum would be accessible via measurements of the Andreev current averaged over a period of driven oscillations. Its differential conductance can detect both the multiharmonic quasiparticle energies, their internal splittings, and probe distribution of the spectral weights in each harmonic.

Furthermore, our study has revealed quite unusual signatures of the superconducting gap threshold Δ. For a sufficiently large amplitude of the oscillations (exceeding the energy gap Δ) there appear incoherent states in the subgap regime, corresponding to short-time living quasiparticles. They emerge predominantly near such values of the amplitude to frequency ratio, where the spectral weight of the zeroth harmonic vanishes. This behavior goes hand in hand with suppression of the on-dot pairing, therefore it should be empirically well detectable in the Josephson-type tunneling configurations. Verification of these predictions should be feasible with the presently available spectroscopic techniques.

Among important unresolved issues one can point out the correlation effects. Mutual interplay between the electron pairing and the Coulomb repulsion might induce a changeover/transition of the ground state between the BCS-like singlet to the spinful doublet configuration, promoting the Kondo effect. Other interesting phenomena could be related to the quasienergies showing up in more complex (for instance three-terminal) junctions [42,43]. These issues, however, are beyond the scope of the present study.

ACKNOWLEDGMENTS

We thank Jens Paaske for useful remarks. This work was supported by the National Science Centre (NCN, Poland) under Grants UMO-2017/27/B/ST3/01911 (B.B.) and UMO-2018/29/B/ST3/00937 (T.D.).

APPENDIX A: FLOQUET APPROACH TO NORMAL QD

Let us consider time-dependent Hamiltonian $H(t) = H(t+T)$, where $T = 2\pi/\omega$ is a period of external driving potential with the characteristic frequency $\omega = 2\pi/T$. Solution of the Schrödinger equation can be formally represented by the Floquet's state $|\Psi_\alpha(t)\rangle = e^{-i\varepsilon_\alpha t}|\Phi_\alpha(t)\rangle$, where $|\Phi_\alpha(t)\rangle$ has the same periodicity T as a perturbation. The wave-function $|\Phi_\alpha(t)\rangle$ obeys the constraint $[H(t) - i\partial_t]|\Phi_\alpha(t)\rangle = \varepsilon_\alpha|\Phi_\alpha(t)\rangle$ with an eigenvalue ε_α [44,45]. In the specialist literature

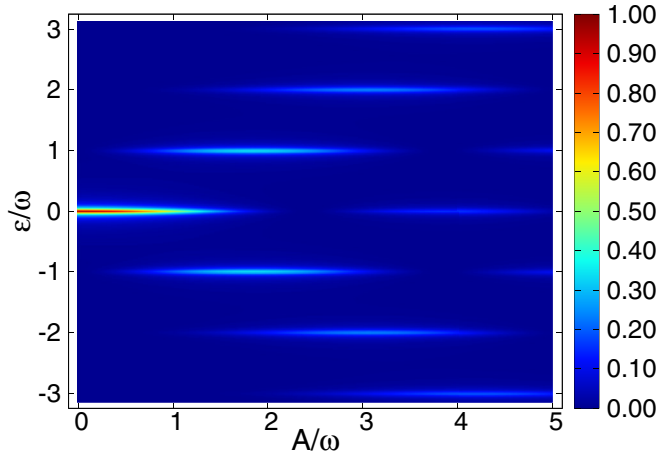

FIG. 11. Quasienergies of the normal quantum dot (coupled to metallic lead by $\Gamma_N/\omega = 0.1$) appearing at $\varepsilon_d \pm l\omega$ and variation of their spectral weights versus the amplitude A of oscillations.

$[H(t) - i\partial_t]$ is dubbed quasioperator and ε_α quasienergy, respectively. In analogy to the Bloch treatment of translationally invariant spacial systems we can restrict to the interval $\varepsilon_\alpha \in [-\omega/2, \omega/2]$, in analogy to the first Brillouin zone. Performing the Fourier expansion of the eigenequation and we get

$$\sum_{m=-\infty}^{\infty} (H_{nm} - n\omega\delta_{nm})|\Phi_{\alpha,m}\rangle = \varepsilon_\alpha|\Phi_{\alpha,n}\rangle, \tag{A1}$$

where the Hamiltonian matrix elements are defined by $H_{nm} = \frac{1}{T}\int_0^T dt e^{i(n-m)\omega t}H(t)$ and the wave function is $|\Phi_{\alpha,m}\rangle = \frac{1}{T}\int_0^T dt e^{in\omega t}|\Phi_\alpha(t)\rangle$. In the extended Hilbert space with a time-independent Hamiltonian this can be written as $|\Psi_\alpha\rangle\rangle = \sum_{n=-\infty}^{\infty}|\Phi_{\alpha,n}\rangle \otimes |n\rangle$. Off-diagonal elements of the Hamiltonian matrix H_{nm} correspond to transition amplitudes between the nth and mth Floquet's modes.

Figure 11 displays typical quasiparticle spectrum of the normal quantum impurity (in the absence of any pairing) driven by the periodic external potential of frequency ω and amplitude A. With increasing amplitude the initial level (here assumed to be $\varepsilon_d = 0$) is replicated at higher harmonics $\varepsilon_d \pm l\omega$. All these quasienergies are characterized by the spectral weights governed by the Bessel functions $J_l(A/\omega)$. They hence reveal a kind of oscillatory variation with respect to A. With an increasing amplitude the spectral weight is shared between more and more harmonic states.

APPENDIX B: MAGNUS EXPANSION

In the high frequency limit one can derive an effective model using the Floquet-Magnus expansion [14,46]. For an illustration of its physical consequences we consider here the deep subgap regime of the QD proximitized to the superconducting lead $H_{QD}^{prox}(t) = H_{QD}(t) + H_{SC} + H_{T,SC}$ which can be approximated by the Hamiltonian

$$H_{QD}^{prox}(t) = \mathcal{H}_0 + \mathcal{V}(t), \tag{B1}$$

where the constant (time-independent) part

$$\mathcal{H}_0 = \varepsilon_d \sum_\sigma d_\sigma^\dagger d_\sigma - (\Delta d_\uparrow^\dagger d_\downarrow^\dagger + \text{H.c.}) \tag{B2}$$

accounts for the induced on-dot pairing $\Delta = \Gamma_S/2$ [39,41] and the periodic perturbation is given by

$$\mathcal{V}(t) = A\sin(\omega t)\sum_\sigma d_\sigma^\dagger d_\sigma. \tag{B3}$$

Within the Floquet's approach the evolution operator over a single driving period

$$U(t_0+T, t_0) = \mathcal{T}_t e^{-i\int_{t_0}^{t_0+T} H_{QD}^{prox}(t)} = e^{-iH_{eff}[t_0]} \tag{B4}$$

(where we set $\hbar \equiv 1$ and $\mathcal{T}_t$ is the chronological ordering operator) can be recast in terms of the effective stroboscopic Hamiltonian $H_{eff}[t_0]$, which formally may depend on choice of the initial time t_0. Restricting to the lowest order expansion terms one obtains [14,46]

$$H_{eff}[t_0] \approx \mathcal{H}_0 + \sum_{l\neq 0}\frac{1}{l\,\omega}(\mathcal{V}_l\mathcal{V}_{-l} + e^{il\omega t_0}[\mathcal{H}_0, \mathcal{V}_l]),$$

where $\mathcal{V}_l$ stands for lth harmonic of the periodic driving potential. This procedure applied to our Hamiltonian (B1)–(B3) yields

$$H_{eff}[t_0] \approx \varepsilon_d \sum_\sigma d_\sigma^\dagger d_\sigma - (\tilde{\Delta} d_\uparrow^\dagger d_\downarrow^\dagger + \tilde{\Delta}^* d_\downarrow d_\uparrow), \tag{B5}$$

with the effective pairing potential

$$\tilde{\Delta} = \Delta\left[1 - \frac{2A}{\omega}\sin(\omega t_0)\right]. \tag{B6}$$

We notice that periodic oscillations of the QD energy level are thus equivalent in the high-frequency regime to rescaling of the induced on-dot pairing potential $\Delta \to \tilde{\Delta}$. The effective quasiparticles of such bilinear Hamiltonian (B5) would hence appear at the energies $\pm\sqrt{\varepsilon_d^2 + |\tilde{\Delta}|^2}$. As a matter of fact, we clearly observe emergence of these two branches accumulating the entire spectral weight in the high frequency limit (see Fig. 3, where we have chosen the Floquet gauge $t_0 = 0$).

[1] A. Mitra, Quantum quench dynamics, Annu. Rev. Condens. Matter Phys. **9**, 245 (2018).
[2] A. Polkovnikov, K. Sengupta, A. Silva, and M. Vengalattore, Colloquium: Nonequilibrium dynamics of closed interacting quantum systems, Rev. Mod. Phys. **83**, 863 (2011).
[3] R. Moessner and S. L. Sondhi, Equilibration and order in quantum Floquet matter, Nat. Phys. **13**, 424 (2017).
[4] T. Oka and S. Kitamura, Floquet engineering of quantum materials, Annu. Rev. Condens. Matter Phys. **10**, 387 (2019).

[5] F. Wilczek, Quantum Time Crystals, Phys. Rev. Lett. **109**, 160401 (2012).

[6] N. Dasari and M. Eckstein, Transient Floquet engineering of superconductivity, Phys. Rev. B **98**, 235149 (2018).

[7] Ch. Georges, J. G. Cosme, L. Mathey, and A. Hemmerich, Light-Induced Coherence in an Atom-Cavity System, Phys. Rev. Lett. **121**, 220405 (2018).

[8] R. Roy and F. Harper, Periodic table for Floquet topological insulators, Phys. Rev. B **96**, 155118 (2017).

[9] J. Klinovaja, P. Stano, and D. Loss, Topological Floquet Phases in Driven Coupled Rashba Nanowires, Phys. Rev. Lett. **116**, 176401 (2016).

[10] T. Čadež, R. Mondaini, and P. D. Sacramento, Edge and bulk localization of Floquet topological superconductors, Phys. Rev. B **99**, 014301 (2019).

[11] M. Sameti and M. J. Hartmann, Floquet engineering in superconducting circuits: From arbitrary spin-spin interactions to the Kitaev honeycomb model, Phys. Rev. A **99**, 012333 (2019).

[12] D. T. Liu, J. Shabani, and A. Mitra, Floquet Majorana zero and π modes in planar Josephson junctions, Phys. Rev. B **99**, 094303 (2019).

[13] M. Grifoni and P. Hänggi, Driven quantum tunneling, Phys. Rep. **304**, 229 (1998).

[14] M. Bukov, L. D'Alessio, and A. Polkovnikov, Universal high-frequency behavior of periodically driven systems: from dynamical stabilization to Floquet engineering, Adv. Phys. **64**, 139 (2015).

[15] P. Titum, E. Berg, M. S. Rudner, G. Refael, and N. H. Lindner, Anomalous Floquet-Anderson Insulator as a Nonadiabatic Quantized Charge Pump, Phys. Rev. X **6**, 021013 (2016).

[16] T. Ozawa, H. M. Price, A. Amo, N. Goldman, M. Hafezi, L. Lu, M. C. Rechtsman, D. Schuster, J. Simon, O. Zilberberg, and I. Carusotto, Topological photonics, Rev. Mod. Phys. **91**, 015006 (2019).

[17] S.-I. Chu and D. A. Telnov, Beyond the Floquet theorem: Generalized Floquet formalisms and quasienergy methods for atomic and molecular multiphoton processes in intense laser fields, Phys. Rep. **390**, 1 (2004).

[18] M. Holthaus, Floquet engineering with quasienergy bands of periodically driven optical lattices, J. Phys. B **49**, 013001 (2015).

[19] S. Kohler, Th. Dittrich, and P. Hänggi, Floquet-Markovian description of the parametrically driven, dissipative harmonic quantum oscillator, Phys. Rev. E **55**, 300 (1997).

[20] G. Platero and R. Aguado, Photon-assisted transport in semiconductor nanostructures, Phys. Rep. **395**, 1 (2004).

[21] N. Goldman and J. Dalibard, Periodically Driven Quantum Systems: Effective Hamiltonians and Engineered Gauge Fields, Phys. Rev. X **4**, 031027 (2014).

[22] A. Eckardt, Colloquium: Atomic quantum gases in periodically driven optical lattices, Rev. Mod. Phys. **89**, 011004 (2017).

[23] N. R. Cooper, J. Dalibard, and I. B. Spielman, Topological bands for ultracold atoms, Rev. Mod. Phys. **91**, 015005 (2019).

[24] L. E. Bruhat, J. J. Viennot, M. C. Dartiailh, M. M. Desjardins, T. Kontos, and A. Cottet, Cavity Photons as a Probe for Charge Relaxation Resistance and Photon Emission in a Quantum Dot Coupled to Normal and Superconducting Continua, Phys. Rev. X **6**, 021014 (2016).

[25] J. Gramich, A. Baumgartner, and C. Schönenberger, Resonant and Inelastic Andreev Tunneling Observed on a Carbon Nanotube Quantum Dot, Phys. Rev. Lett. **115**, 216801 (2015).

[26] L. Arrachea and R. López, Anomalous Joule law in the adiabatic dynamics of a quantum dot in contact with normal-metal and superconducting reservoirs, Phys. Rev. B **98**, 045404 (2018).

[27] Q.-f. Sun, J. Wang, and T.-h. Lin, Resonant Andreev reflection in a normal-metal–quantum-dot–superconductor system, Phys. Rev. B **59**, 3831 (1999).

[28] B. H. Wu, J. C. Cao, and C. Timm, Polaron effects on the dc- and ac-tunneling characteristics of molecular Josephson junctions, Phys. Rev. B **86**, 035406 (2012).

[29] J. Barański and T. Domański, Enhancements of the Andreev conductance due to emission/absorption of bosonic quanta, J. Phys.: Condens. Matter **27**, 305302 (2015).

[30] K. Bocian and W. Rudziński, Phonon-assisted Andreev reflection in a hybrid junction based on a quantum dot, Eur. Phys. J. B **88**, 50 (2015).

[31] Z. Cao, T.-F. Fang, Q.-F. Sun, and H.-G. Luo, Inelastic Kondo-Andreev tunneling in a vibrating quantum dot, Phys. Rev. B **95**, 121110(R) (2017).

[32] R. van Leeuwen, N. E. Dahlen, G. Stefanucci, C.-O. Almbladh, and U. von Barth, Introduction to the Keldysh formalism, in *Time-Dependent Density Functional Theory*, edited by M. A. L. Marques, C. A. Ullrich, F. Nogueira, A. Rubio, K. Burke, and E. K. U. Gross (Springer, Berlin, 2006), pp. 33–59.

[33] N. Tsuji, T. Oka, and H. Aoki, Correlated electron systems periodically driven out of equilibrium: Floquet + DMFT formalism, Phys. Rev. B **78**, 235124 (2008).

[34] D. E. Liu, A. Levchenko, and R. M. Lutchyn, Keldysh approach to periodically driven systems with a fermionic bath: Nonequilibrium steady state, proximity effect, and dissipation, Phys. Rev. B **95**, 115303 (2017).

[35] C. O. Tabarner, Periodically driven S-QD-S junction Floquet dynamics of Andreev bound states, Master Diploma Thesis, University of Copenhagen, 2017.

[36] A. A. M. Cuyt, V. Petersen, B. Verdonk, H. Waadeland, and W. B. Jones, *Handbook of Continued Fractions for Special Functions* (Springer, Berlin, 2008), pp. 345–371.

[37] M. Büttiker, Y. Imry, R. Landauer, and S. Pinhas, Generalized many-channel conductance formula with application to small rings, Phys. Rev. B **31**, 6207 (1985).

[38] Y. Yamada, Y. Tanaka, and N. Kawakami, Interplay of Kondo and superconducting correlations in the nonequilibrium Andreev transport through a quantum dot, Phys. Rev. B **84**, 075484 (2011).

[39] A. Martín-Rodero and A. Levy Yeyati, Josephson and Andreev transport through quantum dots, Adv. Phys. **60**, 899 (2011).

[40] G. S. Uhrig, M. H. Kalthoff, and J. K. Freericks, Positivity of the Spectral Densities of Retarded Floquet Green Functions, Phys. Rev. Lett. **122**, 130604 (2019).

[41] J. Barański and T. Domański, In-gap states of a quantum dot coupled between a normal and a superconducting lead, J. Phys.: Condens. Matter **25**, 435305 (2013).

[42] R. Mélin, J.-G. Caputo, K. Yang, and B. Douçot, Simple Floquet-Wannier-Stark-Andreev viewpoint and emergence of low-energy scales in a voltage-biased three-terminal Josephson junction, Phys. Rev. B **95**, 085415 (2017).

[43] B. Venitucci, D. Feinberg, R. Mélin, and B. Douçot, Nonadiabatic Josephson current pumping by chiral microwave irradiation, Phys. Rev. B **97**, 195423 (2018).

[44] H. Sambe, Steady states and quasienergies of a quantum-mechanical system in an oscillating field, Phys. Rev. A **7**, 2203 (1973).

[45] J. H. Shirley, Solution of the Schrödinger equation with a Hamiltonian periodic in time, Phys. Rev. **138**, B979 (1965).

[46] A. Eckardt and E. Anisimovas, High-frequency approximation for periodically driven quantum systems from a Floquet-space perspective, New J. Phys. **17**, 093039 (2015).